1704
doi:10.1017/S1431927620019030
Microsc. Microanal. 26 (Suppl 2), 2020
© Microscopy Society of America 2020

Imaging Conductivity in a Single Atomic Layer

Ondrej Dyck[1], Jacob Swett[2], Andrew Lupini[1] and Stephen Jesse[1]

[1]Oak Ridge National Laboratory, Oak Ridge, Tennessee, United States, [2]University of Oxford, Alabama, United States

Graphene-based devices are of interest for a wide variety of applications. Many require exquisite control of the atomic structure [1, 2]. The focused probe in a scanning transmission electron microscope (STEM) is well suited for performing precise atomic-scale alterations [3-10]. To leverage this ability for use as a fabrication tool, we have developed a versatile platform to allow *operando* device characterization and modification [11]. This platform connects wafer-scale semiconductor fabrication workflows with STEM-based characterization and e-beam modification as a final fabrication step, allowing operating devices to be examined with atomic resolution. One challenge for imaging a supported graphene device using a STEM is that the substrate (25 nm of SiN in our case) signal overwhelms the signal from the graphene in traditional imaging modes (e.g. HAADF). To address this problem we leverage secondary electron electron-beam induced current (SEEBIC) techniques [12] which reveal interconnected, electrically conductive regions of the device.

Figure 1a shows a diagrammatic representation of the SEEBIC setup used in these experiments. Patterned graphene is electrically connected to Cr/Au contacts on a 25 nm thick SiN window allowing a plan view of the device in STEM. The graphene is grounded through a transimpedance amplifier, the output of which is mapped to the electron beam (e-beam) position on the sample. As the e-beam scans the sample, secondary electrons are ejected and the current needed to neutralize this charge is monitored by the amplifier to give an image. Conductive materials, therefore, appear brighter in the SEEBIC image.

Figure 1b shows a HAADF image of an example, non-operational, graphene nanoribbon device over an aperture in the SiN substrate. Graphene could be seen over the aperture, however, in the supported locations, HAADF imaging was unable to reveal why the device failed or even to detect the graphene. Subsequent SEEBIC imaging of the device, grounding the bottom contact (Figure 1c) and top contact (Figure 1d) reveal very clearly the location of the graphene and where the electrical disconnection is located. The generation of secondary electrons from the 25 nm SiN substrate produces a much higher signal from the supported graphene than from the freestanding regions. Nevertheless, signal is observed from the suspended region. These results demonstrate that SEEBIC imaging can be performed on a single layer of graphene. Figure 1e shows an artificially colored composite image from c and d showing where the electrically conductive and isolated regions meet. The graphene ribbon is broken along the interface with the lower metal contact.

Such *operando* platform, SEEBIC imaging, and STEM-based fabrication hold promise for the fabrication of unique devices capable of harnessing quantum-based properties [13].

https://doi.org/10.1017/S1431927620019030 Published online by Cambridge University Press

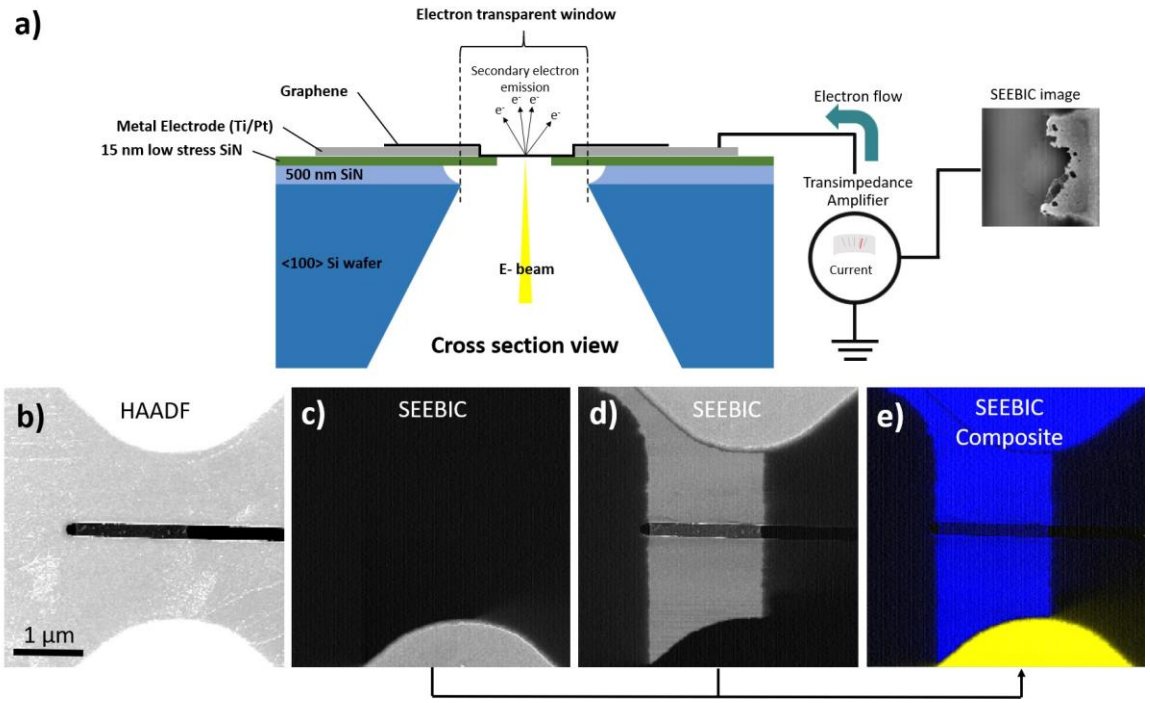

Figure 1. Schematic diagram of the SEEBIC setup and example SEEBIC images. a) Schematic diagram illustrating the configuration for a suspended graphene device and the SEEBIC electrical connections. Supported graphene is not visible through traditional imaging modes (e.g. HAADF) due to the thick substrate, however, the SEEBIC signal is able to clearly reveal the location of the graphene. The SEEBIC micrograph in a) has been filtered for noise. b) HAADF image of a patterned graphene ribbon over an aperture in the SiN substrate. c) and d) corresponding SEEBIC images of the same location as b) with the amplifier connected to either side of the device. We can see there is a break in the graphene ribbon at the lower electrical contact. e) artificially colored composite image of c) and d) together.

References

[1] R Patrik and T Björn, Nanotechnology **21** (2010), p. 302001.
[2] W Han, et al., Nature Nanotechnology **9** (2014), p. 794.
[3] O Dyck, et al., Nature Reviews Materials **4** (2019), p. 497-507.
[4] O Dyck, et al., Applied Physics Letters **111** (2017), p. 113104.
[5] O Dyck, et al., Small **14** (2018), p. 1801771.
[6] O Dyck, et al., Carbon **161** (2020), p. 750-757.
[7] O Dyck, et al., Ultramicroscopy **211** (2020), p. 112949.
[8] T Susi, JC Meyer and J Kotakoski, Ultramicroscopy **180** (2017), p. 163-172.
[9] T Susi, et al., 2D Materials **4** (2017), p. 042004.
[10] M Tripathi, et al., Nano Letters **18** (2018), p. 5319-5323.
[11] JL Swett, et al., Microscopy and Microanalysis **25** (2019), p. 972-973.
[12] M Mecklenburg, et al., Ultramicroscopy **207** (2019), p. 112852.
[13] This work was supported by the U.S. Department of Energy, Office of Science, Basic Energy Sciences, Materials Science and Engineering Division and was performed at the Oak Ridge National Laboratory's Center for Nanophase Materials Sciences (CNMS), a U.S. Department of Energy, Office of Science User Facility.

https://doi.org/10.1017/S1431927620019030 Published online by Cambridge University Press